# Isolating turbulent spots in stratified Plane-Couette flow

John R. Taylor[1], Enrico Deusebio, Colm-cille Caulfield[2,1] and Rich Kerswell[3]

[1] Department of Applied Mathematics and Theoretical Physics, University of Cambridge, Centre for Mathematical Sciences, Willberforce Road, CB3 0WA, Cambridge

[2] BP Institute, University of Cambridge, Madingley Road, CB3 0EZ, Cambridge

[3] School of Mathematics, University of Bristol, BS8 1TW, Bristol

## Abstract

We present a new adaptive control strategy to isolate and stabilize turbulent states in intermittent stably-stratified plane Couette flow in which the gravitational acceleration (non-dimensionalized as the bulk Richardson number $Ri$) is adjusted in time to maintain the turbulent kinetic energy (TKE) of the flow. We demonstrate that applying this method at various stages of decaying stratified turbulence halts the decay process and allows a succession of intermediate turbulent states of decreasing energy to be isolated and stabilized. Once the energy of the initial flow becomes small enough, we identify a single minimal turbulent spot, and lower energy states decay to laminar flow. Interestingly, the turbulent states which emerge from this process have very similar time-averaged $Ri$, but TKE levels different by an order of magnitude. The more energetic states consist of several turbulent spots, each qualitatively similar to the minimal turbulent spot. This suggests that the minimal turbulent spot may well be the lowest energy turbulent state which forms a basic building block of stratified plane Couette flow. The fact that a minimal spot of turbulence can be stabilized so that it neither decays nor grows opens up exciting opportunities for further study of spatiotemporally intermittent stratified turbulence.

## 1 Introduction

Despite the very high Reynolds numbers associated with geophysical flows, turbulence in these flows is often highly intermittent. This is particularly true in stratified boundary layers, where the de-stabilizing influence of shear competes against the stabilizing influence of stratification (e.g. Mahrt, 1999). Direct numerical simulations of canonical wall-bounded stratified flows including channel flow (Flores and Riley (2010); García-Villalba and del Álamo (2011); Brethouwer et al. (2012)), plane Couette flow (García-Villalba et al. (2011); Deusebio et al. (2015)), and stratified boundary layers (Deusebio et al. (2014)) clearly show localized regions of turbulent and laminar flow. Despite the importance of stratified turbulence, the dynamics of these intermittent flows are not well understood.

Recent numerical simulations using a very large horizontal extent have shown that intermittent stratified turbulence can arrange itself into regular patterns consisting of long 'stripes' inclined at an angle in the spanwise direction and localized 'spots' (Brethouwer et al. (2012); Deusebio et al. (2014, 2015)). Similar patterns have been seen in many unstratified transitional flows, albeit at lower Reynolds numbers. For example, in plane Couette flow there is a Reynolds number, $Re_g$, below which the laminar flow is a global attractor but turbulent spots can be triggered transiently (Bottin et al., 1997; Duguet et al., 2010). For Reynolds numbers close to but above $Re_g$, there is a patterned regime where the turbulence arranges itself into regular stripes (e.g. Prigent et al. (2002); Barkley and Tuckerman (2005); Duguet et al. (2010); Manneville (2012)).

Stratification introduces additional parameters, the Richardson number, $Ri$, which quantifies the relative importance of buoyancy compared to shear, and the Prandtl (or Schmidt) number, $Pr = \nu/\kappa$, the ratio of the fluid viscosity to the scalar diffusivity. Here, we use $Ri$ as a control parameter to study spatiotemporal intermittency using direct numerical simulations (DNS) of stratified plane Couette flow. For simplicity, we consider a single $Re = 865$, which is nearly three times larger than the critical value for unstratified plane Couette flow, and $Pr = 0.7$, characteristic of the diffusion of heat in air. In the absence of stratification, flow at this $Re$ would be in the 'featureless' turbulence regime. However, stable stratification retards the transition process and the flow exhibits spatiotemporal intermittency (Deusebio et al. (2015)).

The paper is organized as follows. In section 2.1, we briefly describe the numerical setup and revisit one of the simulations reported in Deusebio et al. (2015) in an intermittent regime, which we use as a baseline simulation. In section 2.2, we describe a series of decay simulations, each of which starts from an initial condition taken from the baseline simulation at $Ri = 0.02$. The decay simulations differ only in the new value of $Ri > 0.02$ subsequently imposed. Section 2.3 then describes a novel strategy to isolate and stabilise a turbulent spot by turning on the dynamic adaption of $Ri$ in the decay simulation for $Ri = 0.05$. The adaptive control procedure allows us to halt the decay process and isolate stripes and spots that characterise intermittent flows with a supercritical transition. Finally, we end with a brief summary and discussion in section 3.

## 2 Results

### 2.1 Setup

Stratified plane-Couette flow is bounded at the top and bottom by flat, rigid plates separated by a distance $2h$. The plates move in opposite directions with constant velocity $\pm U\hat{\mathbf{x}}$. The walls are held at a fixed temperature such that the temperature of the upper wall is $2T$ larger than the lower wall. The flow can be described by three non-dimensional numbers: the Reynolds number, $Re := Uh/\nu$, the bulk Richardson number, $Ri := g\alpha Th/U^2$, and the Prandtl number, $Pr := \nu/\kappa$, where $\nu$ is the kinematic viscosity, $\kappa$ is the thermal diffusivity, $g$ is the gravitational acceleration, and $\alpha$ is the thermal expansion coefficient. Here, $x$, $y$, and $z$ will be used to denote the streamwise, spanwise, and vertical directions, respectively. Periodic boundary conditions are applied in $x$ and $y$, and gravity acts in the $-z$ direction. The numerical code uses a pseudo-spectral method in $x$ and $y$ and second order finite differences to calculate derivatives in the $z$ direction. The timestepping algorithm is a mixed implicit/explicit scheme using the 3rd order Runge-Kutta and Crank-Nicolson methods. Further details of the problem configuration and numerical method can be found in Deusebio et al. (2015).

One of the simulations reported by Deusebio et al. (2015) is chosen as our 'baseline' simulation. This simulation has $Re = 865$, $Ri = 0.02$, and $Pr = 0.7$. Although $Re$ is among the lowest considered by Deusebio et al. (2015), it is still sufficiently high to be in the 'fully turbulent' regime for unstratified plane-Couette flow ($Re \gtrsim 400$) (Duguet et al., 2010). This case was chosen as our baseline since it allows us to use a very large domain in the streamwise and spanwise directions, with $L_x = 64\pi h$ and $L_y = 32\pi h$. The simulation uses 1024 gridpoints in the $x$ and $y$ directions and 64 points in $z$, with gridpoints clustered near both walls. As discussed by Deusebio et al. (2015), the large domain size reduces temporal intermittency of the flow and provides robust statistics.

Panel A of Figure 1(b) shows the streamwise velocity at $z = -0.5h$, the horizontal

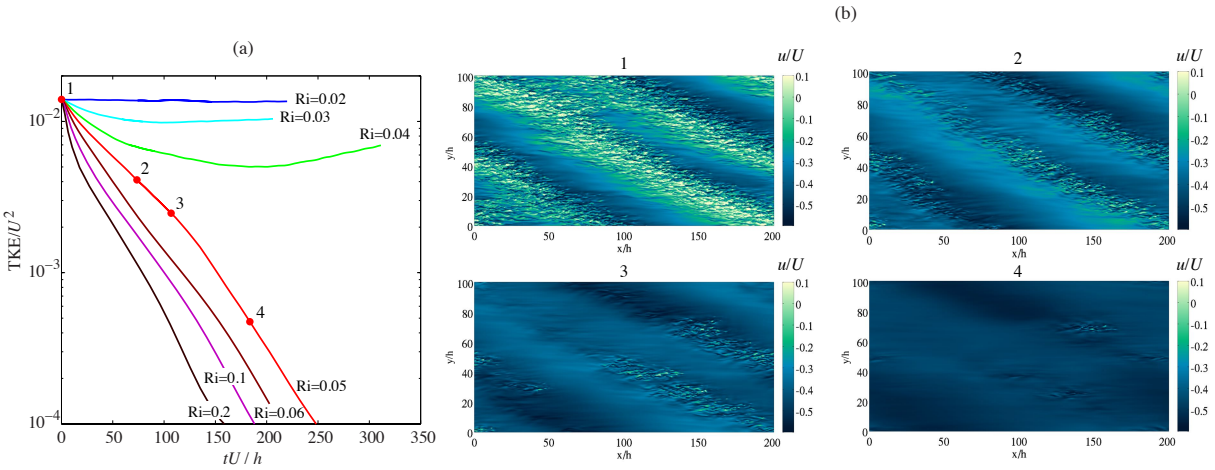


Figure 1: (a) Time series of the turbulent kinetic energy (TKE) in the decay simulations. Each simulation starts from the same initial state labeled A. The Richardson number in each simulation is labeled. (b) Horizontal slices of the streamwise velocity at $z = -0.5h$ at various times in the simulation with $Ri = 0.05$. The corresponding times are indicated with dots and labeled in panel (a).

plane halfway between the lower wall and the centerline. Turbulent and laminar regions develop in inclined bands reminiscent of those seen at lower Reynolds numbers in transitional plane-Couette flow (Prigent et al., 2002). Deusebio et al. (2015) described a method for identifying local turbulent and laminar regions and defined the 'turbulent fraction', $\gamma$, as the ratio of the turbulent and laminar areas of the flow. For sufficiently high $Re$ and $Ri$, the flow is fully turbulent with $\gamma = 1$. Reducing either $Re$ or $Ri$ leads to the onset of intermittency with $0 < \gamma < 1$. For the baseline simulation, $\gamma = 0.64$.

### 2.2 Decay simulations

In the first set of simulations, we varied the strength of the stable stratification by abruptly increasing $Ri$. Each simulation was initialized from the baseline simulation described above with $Re = 865$ and $Ri = 0.02$ with a state obtained at statistical equilibrium. For convenience, $t = 0$ will correspond to the time when $Ri$ is abruptly increased. Since $Ri$ multiplies the buoyancy term in the non-dimensional vertical momentum equation, increasing $Ri$ is equivalent to increasing the gravitational acceleration, i.e. heavy fluid becomes heavier and light fluid becomes lighter.

Figure 1(a) shows the time evolution of the turbulent kinetic energy, TKE $:= \langle \mathbf{u}' \cdot \mathbf{u}' \rangle /2$, where $\langle \cdot \rangle$ denotes a volume average and primes denote a departure from this mean. In four cases with $Ri \geq 0.05$, the TKE decays in time at an approximately exponential rate, and the rate of decay increases with $Ri$. Eventually all simulations with $Ri \geq 0.05$ reach a fully laminar state. When $Ri = 0.03$ and $Ri = 0.04$, the TKE decays during a transient period and partially recovers, but remains below the initial value. For comparison, a continuation of the baseline case with $Ri = 0.02$ is also shown.

The decay process does not proceed uniformly in space, but instead turbulence persists in localized 'bursts'. Figure 1(b) shows four snapshots of the streamwise velocity at $z = -0.5h$ in the decay simulation with $Ri = 0.05$. The corresponding times are indicated using dots in Figure 1(a). Highly localized patches of turbulence can be seen at times labeled 3 and 4, while the rest of the flow is nearly laminar. Qualitatively similar behavior was seen by Manneville (2011) who found breakup of turbulent bands into increasingly localized turbulent patches in decaying unstratified plane-Couette flow.

### 2.3 Adaptive Ri simulations

In order to examine further the influence of stratification on the flow near the laminar-turbulent transition, we have developed a new procedure using the Richardson number, $Ri$, as an adaptive control parameter. The procedure allows us to isolate turbulent states progressively closer to the re-laminarization boundary. The adaptive procedure changes $Ri$ based on the rate of change of TKE. Let $t_0$ correspond to the time $M$ timesteps before the current time, $t$, and let TKE($t_0$) and TKE($t$) be the TKE at these times. The TKE decay rate, $\tau$, between times $t_0$ and $t$ is

$$\tau := \frac{-(t - t_0)}{ln\left(\frac{TKE(t)}{TKE(t_0)}\right)} \tag{1}$$

and the Richardson number, $Ri(t)$, is then set as

$$Ri(t) := Ri(t_0) - c\frac{t - t_0}{\tau} \tag{2}$$

where $Ri(t_0)$ was the previous value at $t_0$. The adaptive $Ri$ procedure acts to maintain a roughly constant value of the TKE. The turbulent fraction and TKE level are sensitive to $Ri$ (Deusebio et al., 2015). During periods where TKE decreases in time ($\tau > 0$), the adaptive procedure will decrease $Ri$ which has the ultimate effect of increasing the TKE, thus leading to the possibility of 'controlling' the turbulence at a nontrivial level. Mathematically, if $Ri$ was adjusted every time step, equations (1) and (2) are a finite difference approximation to imposing the extra dynamical constraint

$$\frac{d}{dt}\left(Ri(t) + c\, ln(TKE)\right) = 0, \tag{3}$$

to the Boussinesq equations ($c = 0$ recovers the Boussinesq equations with constant $Ri$).

In the adaptive Ri simulations, we updated $Ri$ using (2) every $M = 20$ timesteps and set $c = 0.1$. The value of $M$ was chosen to reduce the computational cost of this procedure while ensuring that $Ri$ is adjusted sufficiently often to keep pace with any change in the TKE decay rate. In practice, the time between $Ri$ adjustment steps is always less than one advective unit, $t - t_0 < h/U$. The coefficient $c$ was chosen to ensure that the rate of change in $Ri$ is much less than the TKE decay timescale,

$$\left|\frac{dRi}{dt}\right| \simeq \left|\frac{Ri(t) - Ri_0}{t - t_0}\right| \ll \frac{1}{\tau}. \tag{4}$$

This criterion helps to ensure that the turbulence has time to respond to the changes in $Ri$. We have used the adaptive $Ri$ procedure to isolate turbulent states during various stages of the decay process. We saved 3D flow fields at various times during the decay simulation with $Ri = 0.05$, indicated by dots in Figure 2(a). Each of these was then used as an initial condition for an adaptive $Ri$ simulation. To ensure continuity, $Ri$ was initialized to 0.05 in the adaptive $Ri$ simulations.

Time series of the TKE from the adaptive $Ri$ simulations are shown in dashed lines in Figure 2(a). The decay simulation with $Ri = 0.05$ is shown for reference (solid line). In simulations labeled A-D, the TKE continues to decrease at the start of the adaptive simulation, but soon reaches a quasi-steady state. Simulations initialized later in the decay process have quasi-steady states with lower TKE. Time series of $Ri$ in the adaptive

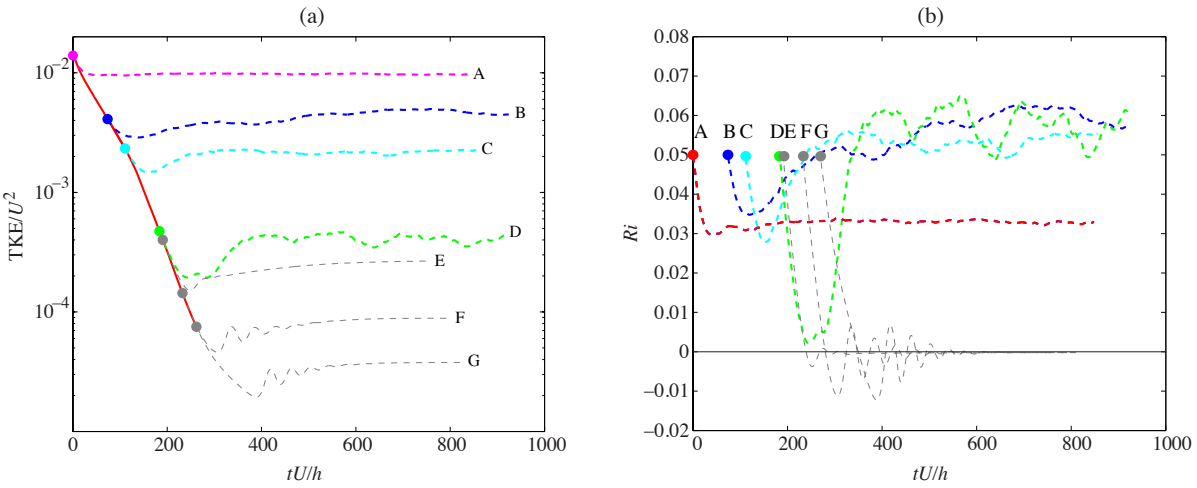


Figure 2: (a) Time series of the turbulent kinetic energy (TKE) in the adaptive Ri simulations. The simulations are initialized from various times in the $Ri = 0.05$ decay simulations as indicated by colored dots. (b) Time series of the Richardson number, $Ri$, for each of the adaptive Ri simulations using the control scheme described in the text. The start time of each simulation is indicated with a colored dot, and the colors and labels are the same as in panel (a)

simulations is shown in Figure 2(b). In all cases $Ri$ reaches a quasi-steady state after an initial drop - mirroring the TKE. Interestingly, the quasi-steady value of $Ri$ in cases B, C, and D falls in the same range, $Ri \simeq 0.05 - 0.06$, despite very different values of the TKE in these simulations. Simulation A has a smaller quasi-steady value of $Ri \simeq 0.03$.

Simulation D is the lowest level of TKE that we have been able to reach using this procedure. In simulations E-G, the flow nearly relaminarizes during the adaptive $Ri$ simulation. In this regime, $Ri$ oscillates and eventually becomes negative (Figure 2b), while the flow develops into a series of streamwise-independent rolls (not shown) corresponding closely to slightly supercritical, sheared Rayleigh-Bénard convection. The character of the flow and the value of the steady state $Ri$ is dramatically different in simulations D and E, implying that the flow in simulation D is close to the re-laminarization boundary.

The streamwise velocity at $z = -0.5h$ is shown for four adaptive Ri simulations in Figure 3. Each snapshot corresponds to the end of the adaptive Ri simulation, as labeled in Figure 2(a). Simulation A was initialized directly from the baseline simulation (magenta dot) with $Ri = 0.05$ and the TKE decreases slightly at the start of the simulation. Turbulent/laminar bands are still prominent features of simulation A, and the laminar regions are more coherent than in the baseline simulation (compare Figure 1b panel 1 and Figure 3 panel A). In the other extreme, simulation D has a single turbulent spot. This spot persists throughout the adaptive Ri simulation, slowly migrating around the domain. Simulations B and C have multiple turbulent spots resembling the one seen in simulation D. In simulation B some of the spots appear to join together with some indications of short inclined bands of turbulence.

The isolated turbulent spot obtained in simulation D is shown in more detail in Figure 4. The upper panel shows the temperature at a horizontal plane passing through $z = -0.5h$, and the lower panel shows a vertical slice through $y = 60h$. Note that the scale of the lower panel has been stretched vertically to help visualize the flow. Turbulence in the spot spans the gap between the lower and upper plates, and is inclined in the direction of plate motion. Small statically unstable regions occur in the turbulent patch.

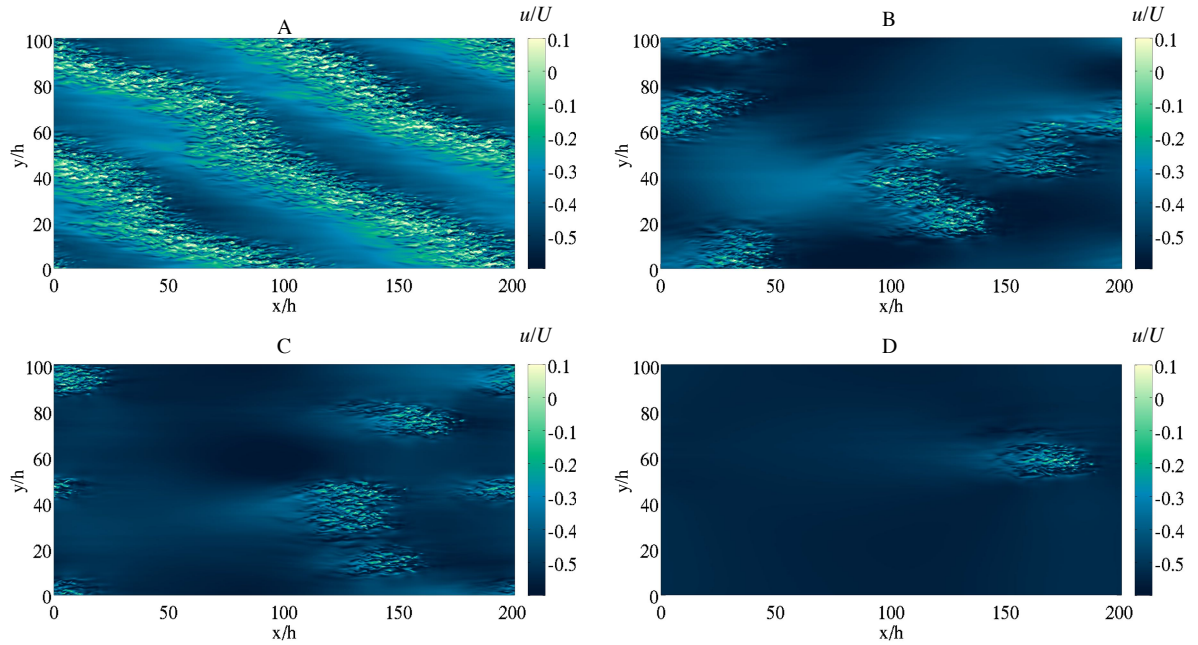


Figure 3: Horizontal slices of the streamwise velocity at $z = -0.5h$ at the end of the adaptive Ri simulations. Labels are the same as in Figure 2.

Undulating features reminiscent of developing Kelvin-Helmholtz billows are visible in the bottom panel between $150 \leq x/h \leq 160$.

Several streamwise streaks are visible within the turbulent spot. The spanwise autocorrelation to the streamwise velocity at the turbulent spot reveals a clear peak in the autocorrelation at a streamwise distance of $\Delta y \simeq 1.67h$. Streamwise streaks are commonly seen in wall-bounded turbulent flows with spanwise spacing between $80\delta_\nu$ and $120\delta_\nu$, where $\delta_\nu = \nu/u_*$ is the viscous lengthscale and $u_* = \sqrt{\tau_w/\rho_0}$ is the friction velocity calculated from the local wall stress, $\tau_w$ (Pope, 2000). Here, since the turbulent spot occupies a small fraction of the domain, the wall stress averaged over the computational domain is close to the corresponding value for purely laminar flow, and the mean friction Reynolds number $Re_* = u_* h/\nu \simeq 29.8$ is only slightly larger than the value for laminar flow at this Reynolds number $Re_*^{lam} = \sqrt{Re} \simeq 29.4$. Using the mean friction Reynolds number gives a streak spacing of 49.8 $\delta_\nu$. However, the friction velocity is higher within the turbulent patch, and the friction Reynolds number based on the local friction velocity reaches values between 50-80. Using these values gives streak spacings between 84-134 wall units, consistent with typical values in wall-bounded turbulence.

## 3 Discussion

We have examined intermittent stratified plane-Couette flow using direct numerical simulations. While the Reynolds number was kept fixed, the Richardson number, $Ri$, was used as a control parameter, allowing us to probe the dynamics of intermittent stratified turbulence in this geometry. We have considered two sets of simulations. In the first set of simulations, $Ri$ is abruptly increased relative to a control simulation. For sufficiently large values of $Ri$, the flow re-laminarizes. However, in these simulations, localized patches of turbulence persist into the decay period until the flow becomes fully laminar. This result is qualitatively similar to Manneville (2011) who found breakup of turbulent bands in

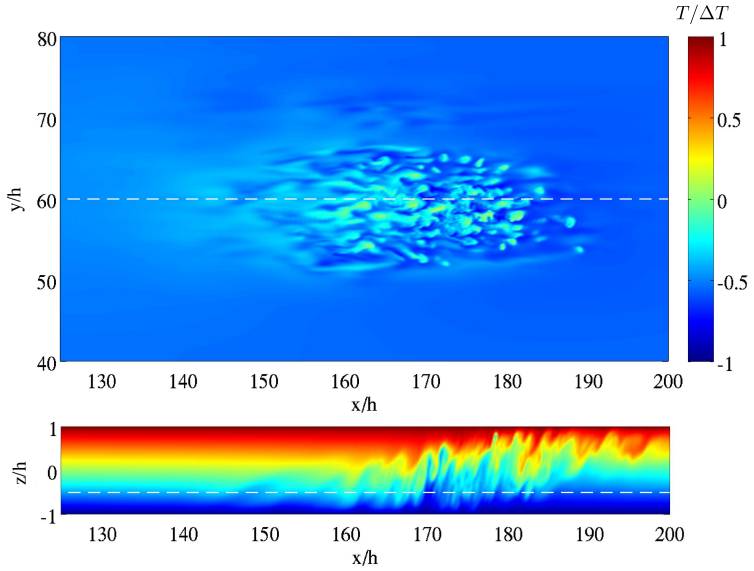


Figure 4: Visualization of the temperature from the end of simulation D for (a) a horizontal plane passing through $z = -0.5h$ (b) a vertical plane passing through $y = 60h$. Only a portion of the simulation domain is shown to highlight the structure of the turbulent spot. The white dashed line in panel (a) indicates the location of the plane shown in panel (b).

decaying unstratified plane-Couette flow.

Next, we describe a new method to isolate flow structures at very low turbulent energy using $Ri$ as an adaptive control parameter. The method adjusts $Ri$ based on the time rate of change in the turbulent kinetic energy (TKE), increasing $Ri$ when the TKE is increasing and lowering $Ri$ when the TKE is decreasing. The adaptive control procedure acts to stabilize the flow close to the initial energy level. By starting the adaptive procedure at various times during a simulation of decaying stratified turbulence, we are able to isolate a variety of low energy flow structures including spots and short stripes of turbulence. The lowest energy turbulent structure that we are able to identify using the adaptive control procedure consists of a single isolated turbulent spot in an otherwise laminar flow.

Here, we have only considered a single Reynolds number, $Re = Uh/\nu = 865$. Although this Reynolds number is large enough to support fully-developed turbulence in the unstratified limit, it is much smaller than typical values in geophysical and industrial flows. One consequence of the moderate Reynolds number is that the Richardson number associated with intermittent flow is also modest. Deusebio et al. (2015) found intermittent behavior at much higher Reynolds numbers for sufficiently large Richardson number, which is also consistent with previous work (e.g. Brethouwer et al., 2012; García-Villalba and del Álamo, 2011; Flores and Riley, 2010). The fate of the laminar-turbulent transition boundary in the limit as $Re \to \infty$ is one of the most important open problems in stratified turbulence. Knowing whether there is a finite 'critical' value of $Ri$ above which turbulence cannot persist as $Re \to \infty$ would be of great use in parameterizing turbulence and mixing in ocean, atmosphere, and climate models.

One of the difficulties with answering this question is the rapid increase in computational cost with increasing $Re$. Very close to the transition boundary, where stratification suppresses energetic turbulence and localizes turbulent patches, the flow might be more accessible to DNS. However, this accessible region narrows in parameter space as $Re \to \infty$ (Deusebio et al., 2015) making it difficult to locate the transition boundary. Here, too our

adaptive control technique might be helpful since the long-time average of $Ri(t)$ needed to maintain a low perturbation energy level as $Re$ increases should be a good predictor for this boundary.

## References


Barkley, D. and Tuckerman, L. S. (2005). Computational study of turbulent laminar patterns in Couette flow. *Phys. Rev. Lett.*, 94(1):014502.

Bottin, S., Dauchot, O., and Daviaud, F. (1997). Intermittency in a locally forced plane Couette flow. *Phys. Rev. Lett.*, 79(22):4377–4380.

Brethouwer, G., Duguet, Y., and Schlatter, P. (2012). Turbulent–laminar coexistence in wall flows with Coriolis, buoyancy or Lorentz forces. *J. Fluid Mech.*, 704:137–172.

Deusebio, E., Brethouwer, G., Schlatter, P., and Lindborg, E. (2014). A numerical study of the unstratified and stratified Ekman layer. *J. Fluid Mech.*, 755:672–704.

Deusebio, E., Caulfield, C. P., and Taylor, J. R. (2015). The intermittency boundary in stratified plane Couette flow. *J. Fluid Mech.*, 781:298–329.

Duguet, Y., Schlatter, P., and Henningson, D. S. (2010). Formation of turbulent patterns near the onset of transition in plane Couette flow. *J. Fluid Mech.*, 650:119.

Flores, O. and Riley, J. J. (2010). Analysis of turbulence collapse in stably stratified surface layers using direct numerical simulation. *Boundary Layer Meteorol.*, 129(2):241–259.

García-Villalba, M., Azagra, E., and Uhlmann, M. (2011). Mixing efficiency in stably-stratified plane Couette flow. *7th Int. Symp. on Stratified flows, Rome, Italy.*

García-Villalba, M. and del Álamo, J. C. (2011). Turbulence modification by stable stratification in channel flow. *Phys. Fluids*, 23(4):045104.

Mahrt, L. (1999). Stratified atmospheric boundary layers. *Boundary-Layer Meteor.*, 90(3):375–396.

Manneville, P. (2011). On the decay of turbulence in plane Couette flow. *Fluid Dyn. Res.*, 43(6):065501.

Manneville, P. (2012). On the growth of laminar–turbulent patterns in plane Couette flow. *Fluid Dyn. Res.*, 44(3):031412.

Pope, S. B. (2000). *Turbulent flows.* Cambridge university press.

Prigent, A., Grégoire, G., Chaté, H., Dauchot, O., and van Saarloos, W. (2002). Large-scale finite-wavelength modulation within turbulent shear flows. *Phys. Rev. Lett.*, 89(1):014501.